Available online at www.sciencedirect.com
ScienceDirect
Journal of Sound and Vibration 324 (2009) 539–555
JOURNAL OF SOUND AND VIBRATION
www.elsevier.com/locate/jsvi

Safety-design criteria of sliding systems for preventing friction-induced vibration

Ken Nakano*, Satoru Maegawa

Graduate School of Environment and Information Sciences, Yokohama National University, 79-7 Tokiwadai, Hodogaya, Yokohama 240-8501, Japan

Received 1 April 2008; received in revised form 14 October 2008; accepted 22 February 2009
Handling Editor: L.G. Tham
Available online 21 April 2009

Abstract

In order to acquire safety-design criteria for preventing friction-induced vibration, dimensionless analysis and numerical simulation have been conducted for a single-degree-of-freedom system with friction. The model includes the discontinuity between static and kinetic friction and the dependence of the kinetic friction coefficient on the relative velocity. Dimensionless description reduces the number of parameters from nine to five; four of the five dimensionless parameters control the occurrence limit of friction-induced vibration. We have derived the occurrence-limit equation on the basis on a previous study on stick–slip in the Coulomb friction model, and we have constructed the discriminant inequalities with the four parameters. They are sufficient conditions for preventing friction-induced vibration, i.e., not only stick–slip but also instability of steady sliding; they are expected to provide safety-design criteria of sliding systems with high usability and high accuracy.

1. Introduction

Almost all mechanical systems utilizing sliding surfaces are designed under the assumption that the surfaces operate smoothly. The generation of friction-induced vibration (FIV) should therefore be estimated and prevented in the design stage of mechanical systems, not only for achieving primary performance, i.e., high function and long lifetime of the mechanical systems, but also for maintaining secondary performance, i.e., comfort for users and the environment without vibration and noise.

For example, when the dependence of the kinetic friction coefficient on the relative velocity is negative, it has been known that steady sliding at the equilibrium point becomes unstable, and the instability leads to the generation of vibration [1]. Consequently, a possible safety-design criterion of the sliding system for preventing vibration would be making the velocity dependence of the kinetic friction coefficient positive; this is often achieved by the development of lubricant and material, e.g., the development of automatic transmission fluids and paper-based material for the suppression of shudder [2–16].

*Corresponding author. Tel./Fax: +81 45 339 4331.
E-mail address: nakano@ynu.ac.jp (K. Nakano).

0022-460X/$ - see front matter © 2009 Elsevier Ltd. All rights reserved.
doi:10.1016/j.jsv.2009.02.027

Nomenclature

a	inverse of the velocity constant (s/m) (Eq. (12))
b	fitting coefficient (Eq. (60))
c	viscous damping coefficient (Ns/m)
F	friction (N)
F_{eq}	friction in the equilibrium state (N) (Eq. (19))
F_k	modulus of kinetic friction (N) (Eqs. (8) and (11))
F_s	static friction (N) (Eq. (4))
$F_{s\max}$	maximum static friction (N) (Eq. (5))
I_1	modified Bessel function of the first kind (Eq. (57))
k	stiffness (N/m)
m	mass of the object (kg)
t	time (s)
V	velocity of the floor surface (m/s)
V_{rel}	relative velocity (m/s) (Eq. (13))
W	contact load (N)
x	position of the object (m)
$\tilde{x}$	position of the object measured from the equilibrium position (m) (Eq. (17))
x_{eq}	equilibrium position of the object (m) (Eq. (18))
α	dimensionless parameter (Eq. (28))
β	instability factor (Eq. (40))
β_{cr}	critical instability factor (Eq. (70))
γ	dimensionless parameter (Eq. (26))
$\Delta\gamma$	dimensionless parameter (Eq. (27))
$\Delta\mu_k$	friction-coefficient difference (Eq. (14))
$\Delta\mu_s$	friction-coefficient difference (Eq. (15))
ζ	dimensionless parameter (damping ratio of the system) (Eq. (25))
ζ_{eff1}	effective damping ratio for $\lambda \ll \lambda_A$ (Eq. (55))
ζ_{eff2}	effective damping ratio for $\lambda \gg \lambda_A$ (Eq. (62))
λ	dimensionless parameter (Eq. (24))
λ_A	constant (Eq. (45))
μ_{eq}	friction coefficient in the equilibrium state (Eq. (19))
μ_k	kinetic friction coefficient (Eq. (12))
μ_{k0}	kinetic friction coefficient for $V_{\mathrm{rel}} = 0$ (Fig. 2)
$\mu_{k\infty}$	kinetic friction coefficient for $V_{\mathrm{rel}} = \infty$ (Fig. 2)
μ_s	static friction coefficient
ξ	dimensionless position of the object (Eq. (22))
$\xi_{s\max}$	maximum of ξ in the stick state (Eq. (33))
$\xi_{s\min}$	minimum of ξ in the stick state (Eq. (32))
σ_1	dimensionless modification factor for $\lambda \ll \lambda_A$ (Eq. (56))
σ_2	dimensionless modification factor for $\lambda \gg \lambda_A$ (Eq. (67))
τ	dimensionless time (Eq. (21))
φ	dimensionless function (Eq. (29))
ω_n	natural frequency of the system (rad/s) (Eq. (23))
$(\dot{})$	derivative with respect to time t
$(')$	derivative with respect to dimensionless time τ

However, this criterion is not sufficient because there is another type of FIV, i.e., stick–slip [17]. The discontinuity between static and kinetic friction is the origin of stick–slip, and the stability of steady sliding is determined regardless of the discontinuity. Consequently, stick–slip is generated if the equilibrium point is stable [18–20], but the instability of steady sliding often leads to stick–slip.

Intrinsically, FIV should be treated as the problem of dynamic systems. Actually, a vast number of studies have been carried out on the FIV in various types of systems. For example, some multi-degree-of-freedom systems were analyzed to know the dynamic behavior of mechanical systems with friction and the occurrence limit of FIV [21–29], and some models were made to know the effect of tangential compliance in contact zones on the dynamics [30–34] including chaos [32]. Moreover, instead of general models, some more practical models, e.g., finite element models, were used to solve problems related to FIV in actual equipments [35–39]. Obviously, such previous studies are worthwhile for individual systems, but a general understanding based on a simple model is also necessary as the basic strategy, not only for tackling unsolved problems but also for preparing for possible problems in newly developed systems.

The stick–slip appearing in a single-degree-of-freedom system with Coulomb friction must be the simplest basic problem. Through the dimensionless analysis of the model, Nakano and Kikuchi found out the existence of two dimensionless parameters controlling the occurrence and non-occurrence of stick–slip [18,19], and Nakano presented a non-occurrence inequality of stick–slip in a power-law form as the sufficient condition

[20]. This inequality has a simple form with high accuracy for usage in the design stage of sliding systems, but it is impossible to express the relationship between instability of steady sliding and stick–slip because it is based on the Coulomb friction model in which the kinetic friction coefficient is assumed to be constant.

The present study is based on the concept of Nakano and Kikuchi [18–20]; the present model has been constructed by considering the dependence of the kinetic friction coefficient on the relative velocity so that it reduces to the Coulomb friction model by setting a dimensionless parameter equal to zero, $\Delta\gamma = 0$. After showing the occurrence limit of FIV obtained by numerical simulation, a set of discriminant inequalities for preventing FIV, Eqs. (71)–(73), will be presented as the safety-design criteria of sliding systems.

2. Modeling

2.1. Analytical model and equation of motion

Fig. 1 shows the analytical model: a single-degree-of-freedom system with friction. A spring k and a dashpot c support an object m, and the object moves in the x direction. The object makes contact with a floor surface moving with a velocity V, and friction F acts on the contact surface. By selecting the origin $x = 0$ at the object position with the natural length of the spring, the equation of motion is given by

$$m\ddot{x} + c\dot{x} + kx = F \tag{1}$$

where $(\dot{})$ denotes the derivative with respect to time t.

There are three types of friction states: stick, slip-I, and slip-II. The friction for each state is described as follows:

- stick state:

$$\dot{x} = V \tag{2}$$

$$F = F_s \tag{3}$$

$$-F_{s\max} \leqslant F_s \leqslant F_{s\max} \tag{4}$$

$$F_{s\max} = \mu_s W \tag{5}$$

- slip-I state:

$$\dot{x} < V \tag{6}$$

$$F = F_k \tag{7}$$

$$F_k = \mu_k W \tag{8}$$

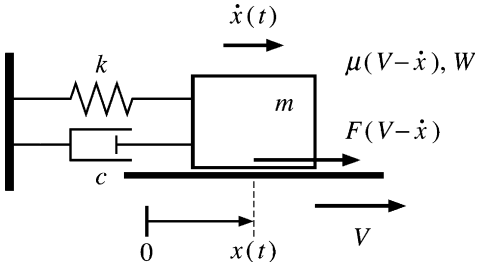

Fig. 1. Analytical model: single-degree-of-freedom system with friction.

- slip-II state:

$$\dot{x} > V \tag{9}$$

$$F = -F_k \tag{10}$$

$$F_k = \mu_k W \tag{11}$$

where F_s is the static friction; $F_{s\max}$, the maximum static friction; F_k, the modulus of kinetic friction; μ_s and μ_k, static and kinetic friction coefficients; and W, the contact load. The velocities of the object and floor surface, $\dot{x}$ and V, respectively, determine which state is realized, as described by Eqs. (2), (6), and (9).

2.2. Dependence of friction coefficient on relative velocity

Fig. 2 shows the dependence of the friction coefficient on the relative velocity. The kinetic friction coefficient is defined as a function of the relative velocity $V_{\rm rel}$:

$$\mu_k = \mu_k(V_{\rm rel}) = \mu_{k0} + \Delta\mu_k(1 - {\rm e}^{-a|V_{\rm rel}|}) \tag{12}$$

where

$$V_{\rm rel} = V - \dot{x} \tag{13}$$

$$\Delta\mu_k = \mu_{k\infty} - \mu_{k0} \tag{14}$$

and a is the inverse of the velocity constant. Note that Fig. 2 is a schematic for $\Delta\mu_k < 0$.

Moreover, the discontinuity between static and kinetic friction is expressed by using

$$\Delta\mu_s = \mu_s - \mu_{k0} \tag{15}$$

$$\mu_s > \mu_{k0} \tag{16}$$

Definitely, we find *nine* independent parameters in the present model: m, c, k, μ_s, μ_{k0}, $\mu_{k\infty}$, a, W, and V. It is, however, not easy to determine the structure of the solutions in nine-dimensional space.

2.3. Dimensionless description

In order to simplify the governing equations, dimensionless variables and parameters are introduced.

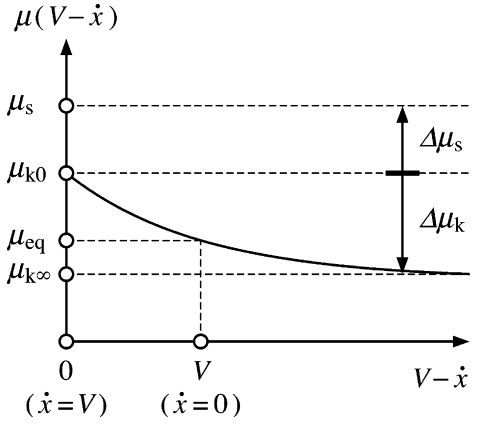

Fig. 2. Dependence of the friction coefficient on the relative velocity.

Before their introduction, the coordinate x is shifted to $\tilde{x}$:

$$\tilde{x} = x - x_{\mathrm{eq}} \tag{17}$$

where

$$x_{\mathrm{eq}} = \frac{F_{\mathrm{eq}}}{k} \tag{18}$$

$$F_{\mathrm{eq}} = \mu_{\mathrm{eq}} W = \mu_k(V) W \tag{19}$$

The subscript "eq" indicates the equilibrium state. By using the new coordinate $\tilde{x}$, the equation of motion is given by

$$m\ddot{\tilde{x}} + c\dot{\tilde{x}} + k\tilde{x} = F - F_{\mathrm{eq}} \tag{20}$$

The dimensionless time τ and dimensionless position ξ are introduced into Eq. (20):

$$\tau = \omega_n t \tag{21}$$

$$\xi = \frac{\omega_n}{V}\tilde{x} \tag{22}$$

where ω_n is the natural frequency of the system:

$$\omega_n = \sqrt{\frac{k}{m}} \tag{23}$$

By using the following dimensionless parameters

$$\lambda = \frac{\Delta\mu_s W}{V\sqrt{mk}} \tag{24}$$

$$\zeta = \frac{c}{2\sqrt{mk}} \tag{25}$$

$$\gamma = \frac{\mu_{k0}}{\Delta\mu_s} \tag{26}$$

$$\Delta\gamma = \frac{\Delta\mu_k}{\Delta\mu_s} \tag{27}$$

$$\alpha = aV \tag{28}$$

and the following dimensionless function

$$\varphi = \varphi(\xi') = \Delta\gamma\lambda(1 - \mathrm{e}^{-\alpha|1-\xi'|}) \tag{29}$$

we obtain the following governing equations in dimensionless form:

- stick state:

$$\xi' = 1 \tag{30}$$

$$\xi_{s\min} \leqslant \xi \leqslant \xi_{s\max} \tag{31}$$

$$\xi_{s\min} = -(1 + 2\gamma)\lambda - 2\zeta - \varphi(0) \tag{32}$$

$$\xi_{s\max} = \lambda - 2\zeta - \varphi(0) \tag{33}$$

- slip-I state:

$$\xi' < 1 \tag{34}$$

$$\xi'' + 2\zeta\xi' + \xi = \varphi(\xi') - \varphi(0) \tag{35}$$

- slip-II state:

$$\xi' > 1 \tag{36}$$

$$\xi'' + 2\zeta\xi' + \xi = -2\gamma\lambda - \varphi(\xi') - \varphi(0) \tag{37}$$

where $(')$ denotes the derivative with respect to dimensionless time τ.

We find that the number of parameters included in the governing equations decreases from *nine* to *five* by using the dimensionless description. The five parameters are defined in Eqs. (24)–(28): λ, ζ, γ, $\Delta\gamma$, and α, and the moving velocity of the floor surface is normalized as shown in Eqs. (30), (34), and (36). Note that the other friction laws are likely to introduce additional dimensionless parameters into the governing equations.

3. Existing criteria

Thus far, there are two known criteria for preventing FIV. One is based on the stability around the equilibrium position, and the other on the occurrence limit of stick–slip with Coulomb friction. In this section, the two criteria are described with the dimensionless parameters defined by Eqs. (24)–(28) as the preparation of the present study.

3.1. Stability limit around equilibrium position

If the equilibrium position is unstable, a disturbance grows and results in self-excited vibration, no matter how small the disturbance is. Consequently, the stability around the equilibrium position is a necessary condition for preventing the FIV.

The function φ is linearized around the equilibrium position $\xi' = 0$:

$$\varphi(\xi') \cong \varphi(0) + \left.\frac{\mathrm{d}\varphi}{\mathrm{d}\xi'}\right|_{\xi'=0} \xi' \tag{38}$$

From Eqs. (35) and (38), we obtain

$$\xi'' + 2(\zeta - \beta\lambda)\xi' + \xi = 0 \tag{39}$$

where

$$\beta = -\tfrac{1}{2}\Delta\gamma\alpha\mathrm{e}^{-\alpha} \tag{40}$$

The stability limit is realized when the coefficient of ξ' is zero, that is,

$$\zeta = \beta\lambda \tag{41}$$

Fig. 3(a) shows the example of the stability limit described by Eq. (41), where $\Delta\gamma$ is changed under $\alpha = 10$. The stability limit is a straight line with a slope of unity in the double-logarithmic plot of λ and ζ. The straight line shifts to the left and the unstable region enlarges as β increases, and thus the parameter β shows the degree of instability.

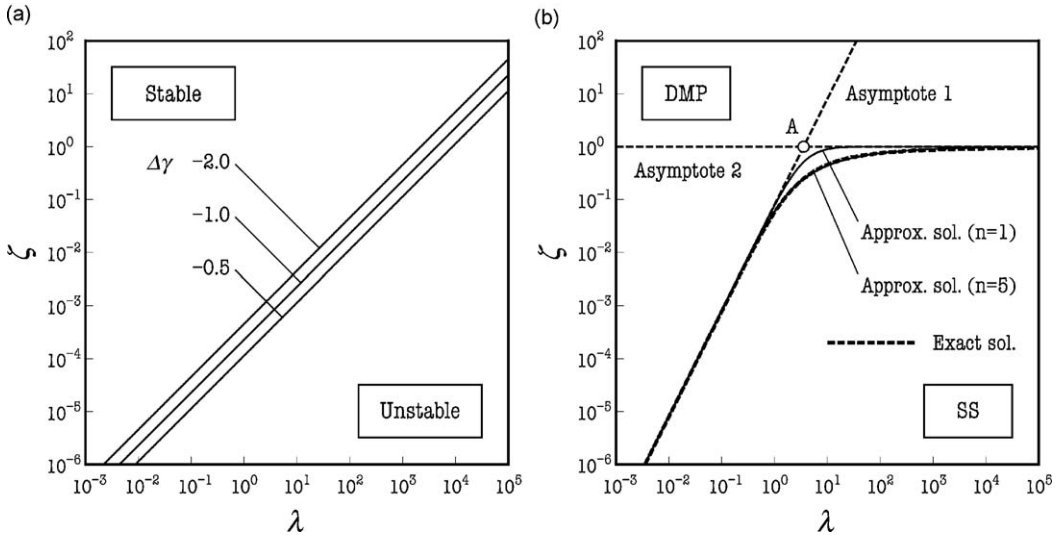

Fig. 3. Existing criteria: (a) the stability limit under $\alpha = 10$ described by Eq. (41); (b) the occurrence limit of stick–slip (SS) in the Coulomb friction model described by Eqs. (42)–(44) and (46).

3.2. Occurrence limit of stick–slip with Coulomb friction

Even if the equilibrium position is stable, the discontinuity between the static and kinetic friction causes stick–slip. When $\Delta\gamma$ is zero, the dependence of the friction coefficient on the relative velocity is eliminated, and Eqs. (30)–(37) reduce to the governing equations for the Coulomb friction model [20].

The occurrence limit of stick–slip with Coulomb friction is obtained by considering the condition where the maximal value of dimensionless velocity in the slip-I state does not reach unity after the stick-to-slip transition. The exact solution of the occurrence limit is given by

$$\ln(1 - 2\zeta\lambda + \lambda^2) = \frac{\zeta}{\sqrt{1-\zeta^2}}\left(3\pi + 2\tan^{-1}\frac{1-\zeta\lambda}{\lambda\sqrt{1-\zeta^2}}\right) \tag{42}$$

and this exact solution has two asymptotes in the double-logarithmic plot of λ and ζ [20], given by

$$\zeta = \frac{1}{4\pi}\lambda^2 \quad \text{for } \lambda \ll \lambda_A \tag{43}$$

$$\zeta = 1 \quad \text{for } \lambda \gg \lambda_A \tag{44}$$

where λ_A is the λ component of the intersecting point A (λ_A, 1) between the two asymptotes:

$$\lambda_A = 2\sqrt{\pi} \tag{45}$$

For Eq. (42), by using the two asymptote Eqs. (43) and (44), an approximate solution is proposed in a power-law form [20]:

$$\frac{(1-\zeta)^n}{\zeta}\lambda^2 = 4\pi \tag{46}$$

The exact solution, asymptotes, and approximate solutions for $n = 1$ and 5 are shown in Fig. 3(b). The two dimensionless parameters, λ and ζ, control the occurrence and non-occurrence of stick–slip with Coulomb friction. The former λ enhances the occurrence of stick–slip, and the latter ζ suppresses it.

4. Numerical simulation

4.1. Method

Based on the dimensionless governing Eqs. (30)–(37), the time evolutions of ξ and ξ' were acquired numerically by using the Runge–Kutta method, in which four different time steps are adopted to guarantee the accuracy of the transition time between the stick and slip states to the order of 10^{-12} [40]. The initial condition was selected at the stick-to-slip transition point: $\xi = \xi_{s\max}$ and $\xi' = 1$.

From the time evolutions, the trajectory was obtained in the dimensionless phase plane, ξ vs. ξ', shown in Fig. 4. Three types of friction states are represented in the plane according to Eqs. (30), (31), (34), and (36); the stick state corresponds with segment PQ on line L ($\xi' = 1$), the slip-I state corresponds with the half plane below L, and the slip-II state corresponds with the half plane above L. Note that point P represents the stick-to-slip transition point, P ($\xi_{s\max}$, 1); if a trajectory meets PQ, the trajectory proceeds to P in the stick state, and the state changes to the slip-I state at P according to the negative acceleration, $\xi''_P = -\lambda < 0$.

4.2. Four types of trajectories

Fig. 5 shows eight examples of time evolutions and trajectories obtained by the numerical simulation. Among the five dimensionless parameters, three are invariants: $\zeta = 0.001$, $\gamma = 2$, and $\alpha = 1$. In Figs. 5(a)–(d), λ is also an invariant: $\lambda = 0.01$. A slow-spiraling trajectory appears in (a) and (b), but a limit cycle appears in (c) and (d). In Figs. 5(e)–(h), λ is unity. A fast-spiraling trajectory appears in (e), but a limit cycle appears in (f)–(h). We can find a tendency that a limit cycle appears for small $\Delta\gamma$.

Through the numerical simulation, we found four types of trajectories shown in Fig. 6. One is for damped motion (DMP): a trajectory from point P spirals in toward the equilibrium point O via the slip-I state, e.g., Figs. 5(a)–(e). The second is for a limit cycle (LC-A): a trajectory from P returns to P via the slip-I and stick states, e.g., Figs. 5(f) and (g). The third is for a limit cycle (LC-B): a trajectory from P returns to P via the slip-I, slip-II, and stick states, e.g., Fig. 5(h). The fourth is for a limit cycle (LC-C): a trajectory from P does not return to P, but a limit cycle is formed outside the segment PQ via the slip-I and slip-II states, e.g., Figs. 5(c) and (d).

Fig. 7 shows the occurrence regions of the four types of trajectories obtained by the numerical simulation under $\zeta = 0.001$, $\gamma = 2$, and $\alpha = 1$. For an invariant λ, the type of trajectory changes in the order of DMP, LC-A, LC-B, and LC-C with decreasing $\Delta\gamma$.

4.3. Occurrence limit of FIV

In the present system, the occurrence of a limit cycle is synonymous with the occurrence of FIV, and the sufficient condition for the non-occurrence of a limit cycle is that the dimensionless velocity ξ' does not reach

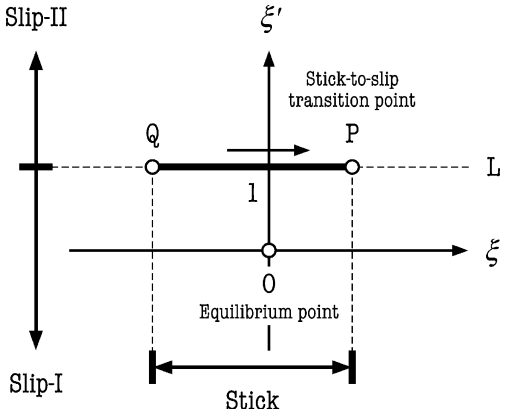

Fig. 4. Dimensionless phase plane and three types of friction states.

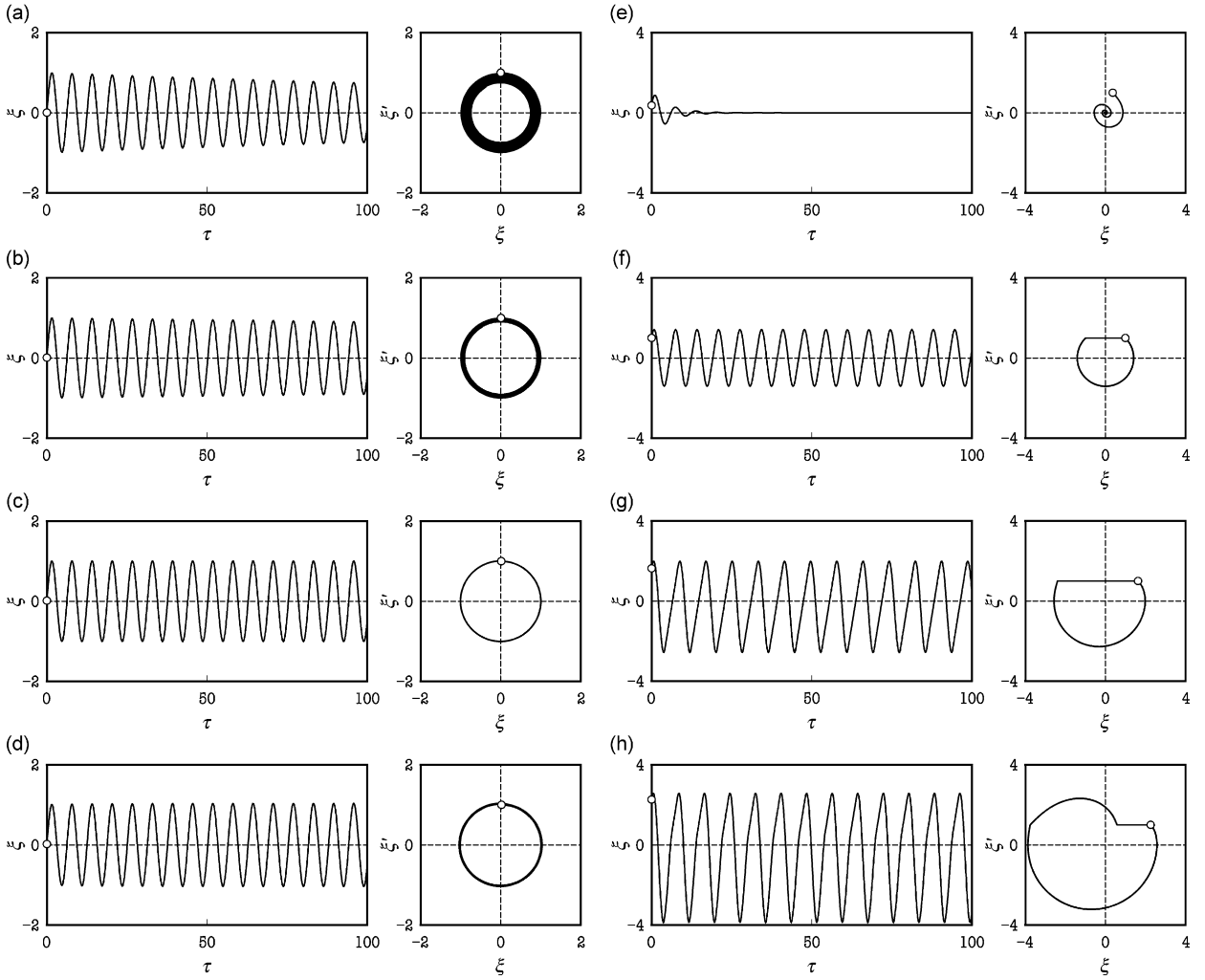

Fig. 5. Numerical results under $\zeta = 0.001$, $\gamma = 2$, and $\alpha = 1$; open circle: initial point (stick-to-slip transition point P): (a) $\lambda = 0.01$, $\Delta\gamma = 1$; (b) $\lambda = 0.01$, $\Delta\gamma = 0$; (c) $\lambda = 0.01$, $\Delta\gamma = -1$; (d) $\lambda = 0.01$, $\Delta\gamma = -2$; (e) $\lambda = 1$, $\Delta\gamma = 1$; (f) $\lambda = 1$, $\Delta\gamma = 0$; (g) $\lambda = 1$, $\Delta\gamma = -1$; (h) $\lambda = 1$, $\Delta\gamma = -2$.

to unity in the slip-I phase starting from the stick-to-slip transition point P. Consequently, the occurrence limit of FIV does not depend on Q ($\xi_{s\min}$, 1), and the minimum necessary equations for finding the occurrence limit of FIV are as follows:

- stick state:

$$\xi' = 1 \tag{47}$$

$$\xi \leqslant \xi_{s\max} \tag{48}$$

- slip-I state:

$$\xi' < 1 \tag{49}$$

$$\xi'' + 2\zeta\xi' + \xi = \varphi(\xi') - \varphi(0) \tag{50}$$

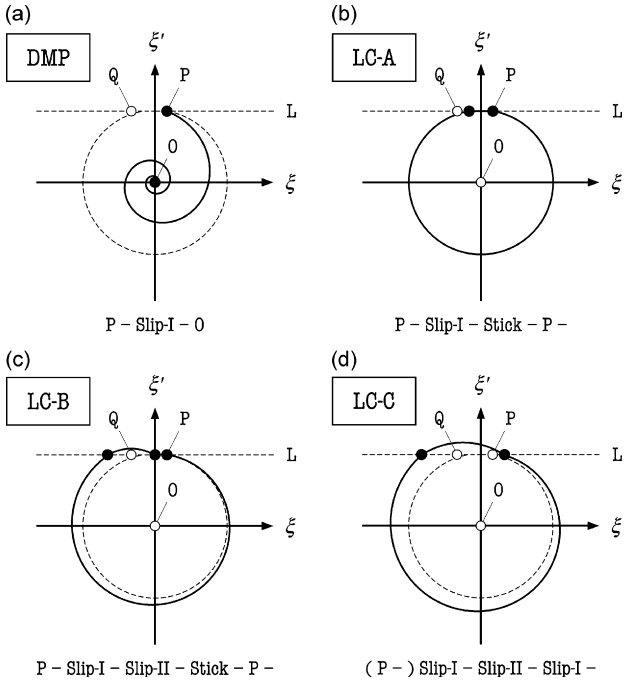

Fig. 6. Typical trajectories of damped motion (DMP) and three types of limit cycles (LC-A, LC-B, and LC-C).

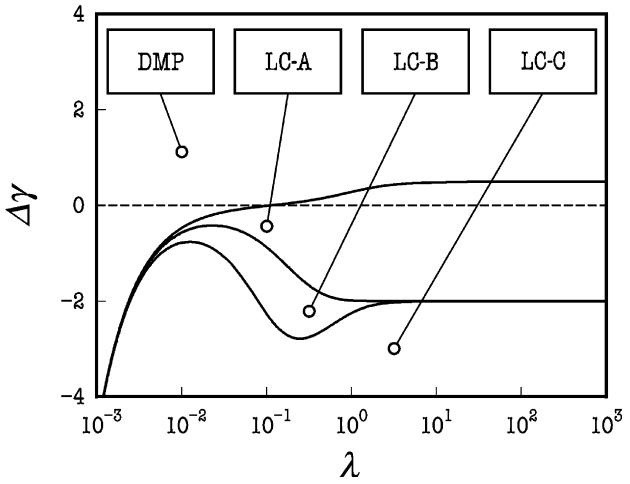

Fig. 7. Occurrence condition of damped motion (DMP) and three types of limit cycles (LC-A, LC-B, and LC-C) under $\zeta = 0.001$, $\gamma = 2$, and $\alpha = 1$.

It should be noted that a dimensionless parameter γ does not appear in Eqs. (47)–(50). This means that the occurrence limit of FIV is determined by *four* dimensionless parameters; they are λ, ζ, $\Delta\gamma$, and α.

Based on Eqs. (47)–(50), we acquired the occurrence limit of FIV numerically. The solid lines in Figs. 8(a)–(c) show the numerical results. A peak with a maximal point at $\lambda = 2.67$ appearing in (a) is lowered in (b) and (c) with increasing α. However, the effect of α on the FIV region is not monotonic; among the three conditions of α in Fig. 8, the FIV region of (b) is the widest for a small λ.

Note that the three solid lines pass through a common point denoted by an open circle in Fig. 8, i.e., $\lambda = 0.112$ and $\Delta\gamma = 0$. This point corresponds to the occurrence limit of the Coulomb friction model; the value of λ is obtained by solving Eq. (42) under $\zeta = 0.001$.

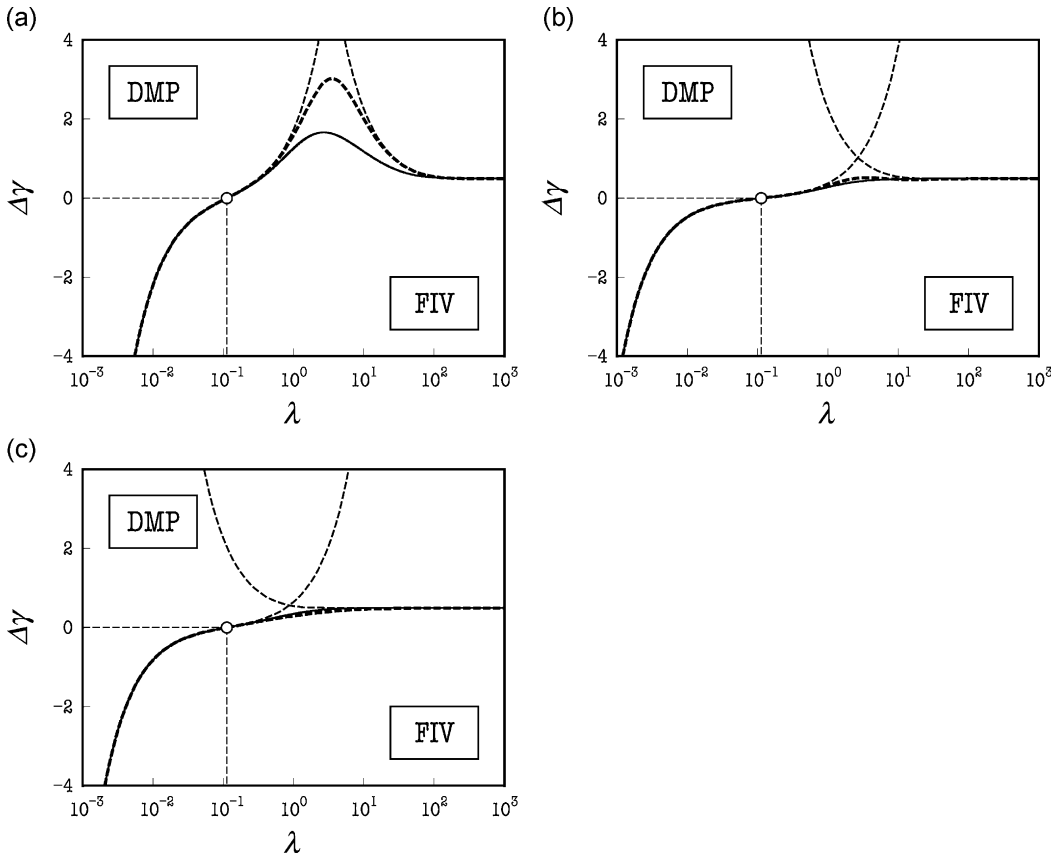

Fig. 8. Occurrence limit of FIV under $\zeta = 0.001$; solid line: numerical results, thin broken lines: occurrence limit described by Eqs. (58) and (66), thick broken line: occurrence limit described by Eq. (69); open circle: occurrence limit for the Coulomb friction model: (a) $\alpha = 0.1$; (b) $\alpha = 1$; (c) $\alpha = 10$.

5. Discriminant inequalities for preventing FIV

The numerical results described in the previous section can be considered as exact solutions, but they are only parts of the infinite solutions generated from the governing equations, Eqs. (30)–(37). The equations include a nonlinear function φ; hence, it is not easy to acquire the exact solution analytically. If it is possible to obtain the exact solution, it must be much more complicated than Eq. (42); furthermore, it would be difficult to expect high usability in a practical sense.

Consequently, in what follows, the occurrence-limit equation in a possible simple form is derived with somewhat rough estimations; the basis is the two asymptotes for the Coulomb friction model, i.e., Eqs. (43) and (44). After deriving the desired equation, its accuracy is examined in comparison with the numerical solutions, and a set of the discriminant inequalities are proposed for preventing FIV.

5.1. Occurrence-limit equation for small λ

In this section, let us consider the case for small λ. Based on Eq. (43) under the assumption of constant kinetic friction coefficient, we assume the following relationship as the occurrence-limit equation:

$$\zeta_{\mathrm{eff}1} = \frac{1}{4\pi}\lambda^2 \quad \text{for } \lambda \ll \lambda_A \tag{51}$$

where $\zeta_{\mathrm{eff}1}$ is the effective damping ratio. In addition, we assume that Eq. (50) reduces to the following form:

$$\xi'' + 2\zeta_{\mathrm{eff}1}\xi' + \xi = 0 \tag{52}$$

By equating the energy dissipations in a period of Eqs. (50) and (52), we obtain

$$\oint \{2\zeta_{\mathrm{eff}1}\xi'\}\,\mathrm{d}\xi = \oint \{2\zeta\xi' - \varphi(\xi') + \varphi(0)\}\,\mathrm{d}\xi \tag{53}$$

At the occurrence limit for $\lambda \ll \lambda_A$, the time evolution of ξ' can be approximated by a sinusoidal function with a unit amplitude and a unit angular frequency [20], e.g., Fig. 5(b):

$$\xi' = \cos\,\tau \tag{54}$$

By executing the integral of Eq. (53) with Eq. (54), we obtain

$$\zeta_{\mathrm{eff}1} = \zeta + \Delta\gamma\sigma_1 \tag{55}$$

where σ_1 is the modification factor from the Coulomb friction model:

$$\sigma_1 = \lambda \mathrm{e}^{-\alpha} I_1(\alpha) \tag{56}$$

The function I_1 is the modified Bessel function of the first kind, which is expressed by an integral form or a series form:

$$I_1(\alpha) = \frac{1}{2\pi}\int_0^{2\pi} \mathrm{e}^{\alpha\cos\,\tau}\cos\,\tau\,\mathrm{d}\tau = \sum_{s=0}^{\infty}\frac{1}{s!(s+1)!}\left(\frac{\alpha}{2}\right)^{2s+1} \tag{57}$$

Consequently, from Eqs. (51) and (55), we obtain the occurrence-limit equation for small λ:

$$\zeta = \frac{1}{4\pi}\lambda^2 - \Delta\gamma\sigma_1 \quad \text{for } \lambda \ll \lambda_A \tag{58}$$

Note that Eq. (58) reduces to Eq. (43) for $\Delta\gamma = 0$.

In Fig. 8, the thin broken line starting from the bottom left shows the occurrence limit expressed by Eq. (58). For small λ, it shows a good agreement with the solid line as the exact solution; we can obtain high accuracy of the occurrence-limit equation, Eq. (58).

5.2. Occurrence-limit equation for large λ

Subsequently, let us consider the occurrence limit of FIV for large λ. Based on Eq. (44), we assume the following relationship as the occurrence-limit equation:

$$\zeta_{\mathrm{eff}2} = 1 \quad \text{for } \lambda \gg \lambda_A \tag{59}$$

where $\zeta_{\mathrm{eff}2}$ is the effective damping ratio. In addition, we assume that $\zeta_{\mathrm{eff}2}$ is expressed by

$$\zeta_{\mathrm{eff}2} = \zeta - \frac{1}{2}\frac{\varphi(1) - \varphi(-b\lambda)}{1 - (-b\lambda)} \tag{60}$$

where b is a fitting coefficient. By neglecting small terms in Eq. (60), we obtain

$$\zeta_{\mathrm{eff}2} = \zeta + \frac{\Delta\gamma}{2b}(1 - \mathrm{e}^{-b\alpha\lambda}) \tag{61}$$

or

$$\zeta_{\mathrm{eff}2} = \zeta + \Delta\gamma\sigma_2 \tag{62}$$

where σ_2 is the modification factor from the Coulomb friction model. From Eqs. (59) and (61), we obtain

$$\lim_{\lambda\to\infty}\Delta\gamma = 2b(1 - \zeta) \tag{63}$$

On the other hand, through the numerical simulation, we found that $\Delta\gamma$ at the occurrence limit is roughly approximated by

$$\lim_{\lambda\to\infty}\Delta\gamma \cong \tfrac{1}{2}(1-\zeta) \quad \text{for } 0<\zeta<1 \tag{64}$$

From Eqs. (63) and (64), we obtain the value of b:

$$b = \tfrac{1}{4} \tag{65}$$

Consequently, from Eqs. (59), (61), (62), and (65), we obtain the occurrence-limit equation for large λ in the following form:

$$\zeta = 1 - \Delta\gamma\sigma_2 \quad \text{for } \lambda \gg \lambda_A \text{ and } 0<\zeta<1 \tag{66}$$

where

$$\sigma_2 = 2(1-\mathrm{e}^{-\alpha\lambda/4}) \tag{67}$$

Note that Eq. (66) reduces to Eq. (44) for $\Delta\gamma = 0$.

In Fig. 8, the thin broken line toward the middle right shows the occurrence limit expressed by Eq. (66). For large λ, it shows a good agreement with the solid line as the exact solution; we can obtain high accuracy of the occurrence-limit equation, Eq. (66).

5.3. Occurrence-limit equation in integrated form

The occurrence-limit equation integrating Eqs. (55) and (62) is obtained on the basis of Eq. (46) for $n = 1$:

$$\frac{1-\zeta_{\mathrm{eff}2}}{\zeta_{\mathrm{eff}1}}\lambda^2 = 4\pi \tag{68}$$

From Eqs. (55), (62), and (68), we arrive at

$$(1-\zeta)\lambda^2 - 4\pi\zeta = \Delta\gamma(4\pi\sigma_1 + \lambda^2\sigma_2) \quad \text{for } 0<\zeta<1 \tag{69}$$

Note that Eq. (69) reduces to Eq. (46) for $\Delta\gamma = 0$.

In Fig. 8, the thick broken line shows the occurrence limit expressed by Eq. (69). Since it is acquired on the basis of Eqs. (55) and (62) for small and large λ, respectively, it reduces to the two thin broken lines for $\lambda \ll \lambda_A$ and $\lambda \gg \lambda_A$, and shows a good agreement with the exact solution. An inaccurate prediction is found for intermediate values of λ, especially for small α as shown in Fig. 8(a), which might be caused by the function σ_2 in which the two parameters exist only as their product $\alpha\lambda$; by decreasing the value of $\alpha\lambda$, small α degrades the accuracy of Eqs. (62) and (69) including the function σ_2.

5.4. Proposed discriminant inequalities as sufficient conditions

By integrating the stability limit around the equilibrium point, Eq. (41), and the occurrence limit of FIV starting from the stick-to-slip transition point, Eq. (69), we obtain the discriminant inequalities for preventing FIV. By considering that the stability-limit equation, Eq. (41), passes through point A shown in Fig. 3(b) when $\beta = \beta_{\mathrm{cr}}$

$$\beta_{\mathrm{cr}} = \frac{1}{\lambda_A} = \frac{1}{2\sqrt{\pi}} \tag{70}$$

the discriminant inequalities can be described as follows:

- $\beta > \beta_{\mathrm{cr}}$:

$$\zeta > \beta\lambda \tag{71}$$

- $\beta<\beta_{cr}$:

$$\zeta>\beta\lambda \quad \text{for } \zeta>0 \tag{72}$$

$$(1-\zeta)\lambda^2-4\pi\zeta<\Delta\gamma(4\pi\sigma_1+\lambda^2\sigma_2) \quad \text{for } 0<\zeta<1 \tag{73}$$

It should be noted that the discriminant inequalities are the *sufficient conditions* for preventing FIV, which are suitable for the safety-design criteria of sliding systems.

For $\beta>\beta_{cr}$, the stability around the equilibrium point, Eq. (71), is the necessary and sufficient condition because the stability limit exceeds the occurrence limit of FIV. On the other hand, for $\beta<\beta_{cr}$, the stability condition is necessary but not sufficient, and the additional condition, Eq. (73), is also necessary. When Eq. (72) is satisfied but Eq. (73) is not satisfied, smooth sliding motion is realized at the equilibrium point, but a disturbance, e.g., unexpected impulsive force, causes FIV. In contrast, if Eqs. (72) and (73) are satisfied

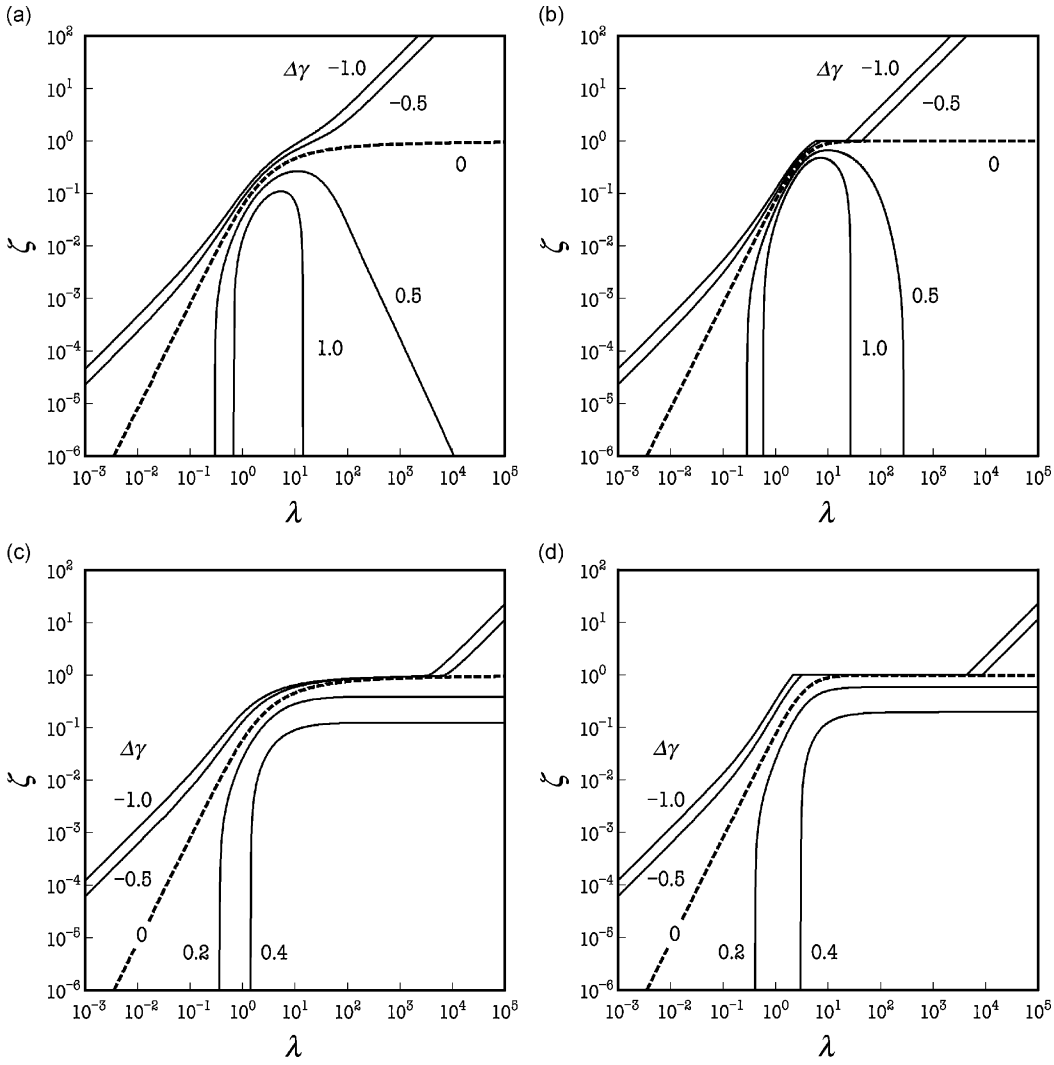

Fig. 9. Comparison between the numerical simulation and proposed discriminant inequalities (Eqs. (71)–(73)) with respect to the occurrence limit of FIV; broken line: occurrence limit for the Coulomb friction model ($\Delta\gamma=0$): (a) numerical simulation under $\alpha=0.1$; (b) proposed discriminant inequalities under $\alpha=0.1$; (c) numerical simulation under $\alpha=10$; (d) proposed discriminant inequalities under $\alpha=10$.

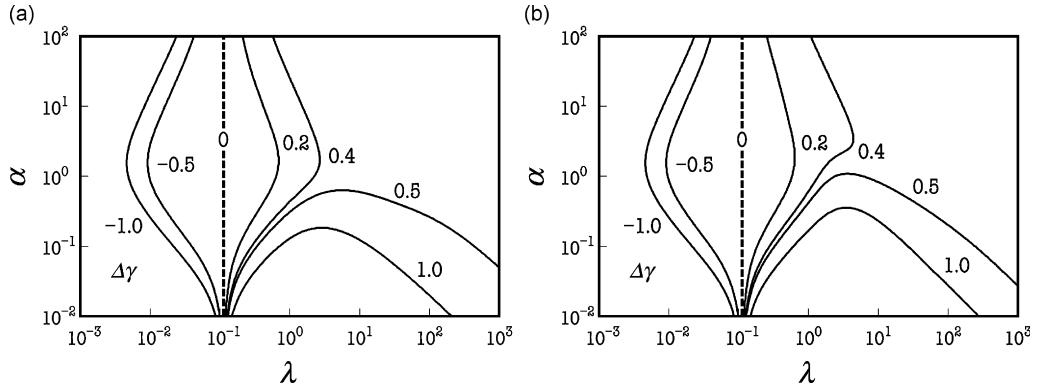

Fig. 10. Comparison between the numerical simulation and proposed discriminant inequalities (Eqs. (71)–(73)) with respect to the occurrence limit of FIV; broken line: occurrence limit for the Coulomb friction model ($\Delta\gamma = 0$): (a) numerical simulation under $\zeta = 0.001$; (b) proposed discriminant inequalities under $\zeta = 0.001$.

simultaneously, the effective damping of the system is enough to dissipate the energy of such a disturbance, and smooth sliding motion is ensured.

The accuracy of the proposed discriminant inequalities was examined in other cross sections of the structure of solutions. Figs. 9 and 10 show the comparison between the numerical simulation and proposed discriminant inequalities with respect to the occurrence limit of FIV in the λ vs. ζ plane and λ vs. α plane, respectively. The occurrence limit changes with varying $\Delta\gamma$ from the broken line representing the Coulomb friction model, $\Delta\gamma = 0$. We can confirm that the proposed discriminant inequalities have the ability to extensively predict the conditions for preventing FIV.

6. Conclusions

(1) For the exponential friction law used in the present system, there are five dimensionless parameters (λ, ζ, γ, $\Delta\gamma$, and α defined by Eqs. (24)–(28)) determining the dynamics of a sliding system considering the discontinuity between static and kinetic friction and the dependence of the kinetic friction coefficient on the relative velocity. Among the five parameters, γ does not affect the occurrence limit of friction-induced vibration (FIV).

(2) There are three types of FIV. One is via the stick and slip-I states (LC-A); the second is via stick, slip-I, and slip-II states (LC-B); and the third is via slip-I and slip-II states (LC-C). The occurrence limit of LC-A determines the occurrence limit of the FIV.

(3) The proposed discriminant inequalities (Eqs. (71)–(73)) are described with four dimensionless parameters (λ, ζ, $\Delta\gamma$, and α); they are the sufficient conditions for preventing FIV considering the stability limit around the equilibrium point and the occurrence limit of FIV starting from the stick-to-slip transition point.

Acknowledgment

The authors would like to express their sincere thanks to Prof. Takahiro Kondou at Kyushu University for fruitful discussions on the exact solution for the Coulomb friction model, Eq. (42).

References

[1] J.P. Den Hartog, *Mechanical Vibration*, fourth ed., McGraw-Hill, New York, 1956.

[2] M. Eguchi, T. Miyazaki, T. Yamamoto, Boundary friction characteristic of wet friction materials (part 1)—tangential displacement behavior under constant tangential loading conditions, *Journal of Japanese Society of Tribologists* 39 (1994) 160–167.

[3] M. Eguchi, T. Miyazaki, T. Yamamoto, Boundary friction characteristic of wet friction materials (part 2)—consideration on boundary friction–velocity characteristics by coefficient of tangential force–velocity relationship obtained under the conditions of constant tangential loading, *Journal of Japanese Society of Tribologists* 39 (1994) 168–175.
[4] H. Ohtani, R.J. Hartley, D.W. Stinnett, Prediction of the anti-shudder properties of automatic transmission fluids using a modified SAE no. 2 machine, *SAE Transactions* 103 (1994) 456–467.
[5] C.G. Slough, M.P. Everson, R.C. Jaklevic, D.J. Melotik, W. Shen, Clutch shudder correlated to ATF degradation through local friction vs. velocity measurements by a scanning force microscope, *Tribology Transactions* 39 (1996) 609–614.
[6] Y. Kato, R. Akasaka, T. Yamazaki, Study on origin of shudder under slip control of a lock-up clutch in an automatic transmission (part 1)—measurement of friction characteristics under shudder, *Journal of Japanese Society of Tribologists* 42 (1997) 485–491.
[7] R.F. Watts, R.K. Nibert, M. Tandon, Anti-shudder durability of automatic transmission fluids: mechanism of the loss of shudder control, *Tribotest* 4 (1997) 29–50.
[8] Y. Kato, R. Akasaka, T. Yamazaki, Study on origin of shudder under slip control of a lock-up clutch in an automatic transmission (part 2)—relationship between friction characteristics under shudder and adsorption of additives, *Journal of Japanese Society of Tribologists* 43 (1998) 309–316.
[9] M.P. Everson, H. Ohtani, New opportunities in automotive tribology, *Tribology Letters* 5 (1998) 1–12.
[10] T. Kugimiya, N. Yoshimura, J. Mitsui, Tribology of automatic transmission fluid, *Tribology Letters* 5 (1998) 49–56.
[11] M. Tohyama, T. Ohmori, S. Sanda, F. Ueda, Anti-shudder mechanism of ATF additives (part 1)—formation of contact area roughness, *Journal of Japanese Society of Tribologists* 47 (2002) 565–574.
[12] M. Tohyama, T. Ohmori, S. Sanda, F. Ueda, Anti-shudder mechanism of ATF additives (part 2)—influence of boundary frictional property and contact area roughness, *Journal of Japanese Society of Tribologists* 47 (2002) 575–581.
[13] S. Li, M.T. Devlin, S.H. Tersigni, T.C. Jao, K. Yatsunami, T.M. Cameron, Fundamentals of anti-shudder durability: part I—clutch plate study, *SAE Transactions* 112 (2003) 1846–1857.
[14] Y. Sambongi, T. Shibuya, S. Morishita, Vibration in wet friction systems with paper-based material, *Journal of Japanese Society of Tribologists* 49 (2004) 163–172.
[15] R. Maki, B. Ganemi, E. Hoglund, R. Olsson, Wet clutch transmission fluid for AWD differentials: influence of lubricant additives on friction characteristics, *Lubrication Science* 19 (2006) 87–99.
[16] P. Nyman, R. Maki, R. Olsson, B. Ganemi, Influence of surface topography on friction characteristics in wet clutch applications, *Wear* 261 (2006) 46–52.
[17] F.P. Bowden, D. Tabor, *The Friction and Lubrication of Solids*, Oxford University Press, New York, 1950.
[18] K. Nakano, Y. Kikuchi, Conditional expression for the occurrence of stick–slip motion based on the Coulomb friction model (part 1)—formulation and approximation of conditional expression, *Journal of Japanese Society of Tribologists* 51 (2006) 131–139.
[19] K. Nakano, Y. Kikuchi, Conditional expression for the occurrence of stick–slip motion based on the Coulomb friction model (part 2)—examination of conditional expression and proposal of simplified expression, *Journal of Japanese Society of Tribologists* 51 (2006) 140–146.
[20] K. Nakano, Two dimensionless parameters controlling the occurrence of stick–slip motion in a 1-DOF system with Coulomb friction, *Tribology Letters* 24 (2006) 91–98.
[21] T.K. Pratt, R. Williams, Non-linear analysis of stick/slip motion, *Journal of Sound and Vibration* 74 (1981) 531–542.
[22] M.T. Bengisu, A. Akay, Stability of friction-induced vibration in multi-degree-of-freedom systems, *Journal of Sound and Vibration* 171 (1994) 557–570.
[23] B. Wikiel, J.M. Hill, Stick–slip motion for two coupled masses with side friction, *International Journal of Non-Linear Mechanics* 35 (2000) 953–962.
[24] U. Galvanetto, Some discontinuous bifurcations in a two-block stick–slip system, *Journal of Sound and Vibration* 248 (2001) 653–669.
[25] F. Xia, Modelling of a two-dimensional Coulomb friction oscillator, *Journal of Sound and Vibration* 265 (2003) 1063–1074.
[26] E.J. Berger, C.M. Krousgrill, F. Sadeghi, Friction-induced sliding instability in a multi-degree-of-freedom system with oscillatory normal forces, *Journal of Sound and Vibration* 266 (2003) 369–387.
[27] N.M. Kinkaid, O.M. O'Reilly, P. Papadopoulos, On the transient dynamics of a multi-degree-of-freeedom friction oscillator: a new mechanism for disc brake noise, *Journal of Sound and Vibration* 287 (2005) 901–917.
[28] C. Wensrich, Slip–stick motion in harmonic oscillator chains subject to Coulomb friction, *Tribology International* 39 (2006) 490–495.
[29] M.N.A. Emira, Friction-induced oscillations of a slider: parametric study of some system parameters, *Journal of Sound and Vibration* 300 (2007) 916–931.
[30] B.N.J. Persson, Theory of friction: the role of elasticity in boundary lubrication, *Physical Review B* 50 (1994) 4771–4786.
[31] A.J. McMillan, A non-linear friction model for self-excited vibrations, *Journal of Sound and Vibration* 205 (1997) 323–335.
[32] N. Hinrichs, M. Oestreich, K. Popp, On the modelling of friction oscillators, *Journal of Sound and Vibration* 216 (1998) 435–459.
[33] C.M. Jung, Friction-induced vibration in periodic linear elastic media, *Journal of Sound and Vibration* 252 (2002) 945–954.
[34] J. Slavic, M.D. Bryant, M. Boltezar, A new approach to roughness-induced vibrations on a slider, *Journal of Sound and Vibration* 306 (2007) 732–750.
[35] H. Ouyang, J.E. Mottershead, Unstable traveling waves in the friction-induced vibration of discs, *Journal of Sound and Vibration* 248 (2001) 768–779.
[36] M. Paliwal, A. Mahajan, J. Don, T. Chu, P. Filip, Noise and vibration analysis of a disc-brake system using a stick–slip friction model involving coupling stiffness, *Journal of Sound and Vibration* 282 (2005) 1273–1284.
[37] J. Huang, C.M. Krousgrill, A.K. Bajaj, Modeling of automotive drum brakes for squeal and parameter sensitivity analysis, *Journal of Sound and Vibration* 289 (2006) 245–263.

[38] S. Lignon, J.J. Sinou, L. Jezequel, Stability analysis and μ-synthesis control of brake systems, *Journal of Sound and Vibration* 298 (2006) 1073–1087.
[39] G.X. Chen, Q.Y. Liu, X.S. Jin, Z.R. Zhou, Stability analysis of a squealing vibration model with time delay, *Journal of Sound and Vibration* 311 (2008) 516–536.
[40] G. Cheng, J.W. Zu, Dynamics of a dry friction oscillator under two-frequency excitations, *Journal of Sound and Vibration* 275 (2004) 591–603.